

# Multilinear Sparse Decomposition for Best Spectral Bands Selection

Hamdi Jamel Bouchech<sup>1,2</sup>, Sebti Foufou<sup>2,1</sup>, and Mongi Abidi<sup>3</sup>

<sup>1</sup> LE2i Lab., University of Burgundy, Dijon, France

<sup>2</sup> Computer Science and Engineering, CENG, P.O. Box 2713,  
Qatar University Doha, Qatar

<sup>3</sup> IRIS Lab, Dept of Elec.Eng and Comp.Sci, University of Tennessee,  
Knoxville, TN, USA

**Abstract.** Optimal spectral bands selection is a primordial step in multispectral images based systems for face recognition. In this context, we select the best spectral bands using a multilinear sparse decomposition based approach. Multispectral images of 35 subjects presenting 25 different lengths from 480nm to 720nm and three lighting conditions: fluorescent, Halogen and Sun light are grouped in a 3-mode face tensor  $T$  of size  $35 \times 25 \times 2$ .  $T$  is then decomposed using 3-mode SVD where three mode matrices for subjects, spectral bands and illuminations are sparsely determined. The  $25 \times 25$  spectral bands mode matrix defines a sparse vector for each spectral band. Spectral bands having the sparse vectors with the lowest variation with illumination are selected as the best spectral bands. Experiments on two state-of-the-art algorithms, MBLBP and HGPP, showed the effectiveness of our approach for best spectral bands selection.

**Keywords:** Spectral bands, Multilinear, sparse, Tensor, MBLBP, HGPP.

## 1 Introduction

Face recognition is proved to be a challenging and ill posed task encountered in several real life applications. Several highly uncontrolled parameters are involved in such task. The most important of these parameters are those related to the imaging conditions like illumination, pose, and aging [7] [8] [9]. Specifically, the illumination factor is one of the most critical of these parameters. It has been widely addressed by researcher. In [12], algorithms of more than 99% accuracy on normal face images from the FERET database (Fb image set), do not surpass 80% when tested on images with high illumination variation from the CAS-PEAL-R1 face database. In [10], extensive experiments have been conducted to study the effect of illumination variation on state-of-the-art algorithms like MBLBP [13] HGPP [12] and POEM [14]. Unsatisfactory results have been reported with 62.9 % maximum accuracy on the CAS-PEAL-R1 face database and 65.4% accuracy upon the HFB face database [15]. The later database presents images from the NIR and Visible spectrums that were matched against each others. To build illumination invariant systems that are robust against high illumination variation,

several research groups have proposed to use images captured at different wavelengths of the light spectrum including NIR, LWIR, SWIR, and thermal images. The partial complementarity of these wavelengths have been investigated and multimodal information were then extracted and fused in different ways. In [20], the authors proposed to use images captured at multiple wavelengths of the visible spectrum. Fluorescent, halogen and day lighted multispectral images ranging from 480nm to 720nm, with a step of 10nm (providing 25 spectral bands per subject), were then captured and grouped in one database called IRIS-M<sup>3</sup>. Several matching scenarios between lighting modalities including halogen vs fluorescent, Halogen vs day light and fluorescent vs day light face matching, were then experimented. Reported results showed the capacity of these multispectral images to reduce the problem of matching day lighted faces. Using all the 25 visible spectral bands provided for each subject is both source consuming and not efficient. To solve this problem, Bouchech et al. proposed two approaches to select the best spectral bands for face matching. The approach in [21] selects the same optimal spectral bands for all subjects (static best spectral bands selection SBSS) using a pursuit optimization formulation, while the second approach [22] selects different spectral bands for each subject (dynamic best spectral bands selection DBSS) using mixture of Gaussian and likelihood ratio test. Only selected bands were then used for face matching and the proposed two systems achieved better performance than systems based on broad band images.

In this paper, we propose a different static approach for best spectral bands selection. All Multispectral images provided by the IRIS-M<sup>3</sup> face database are superposed in a 3-mode face tensor  $T$  of size  $35 \times 25 \times 2$  corresponding to 35 subjects, 25 spectral bands and two modalities from the three modalities available in the database.  $T$  is then decomposed as  $T = Z \times U_{subject} \times U_{spectralbands} \times U_{illumination}$  using the domain adaptive dictionaries learning (DADL) algorithm proposed in [23]. The obtained  $25 \times 25$  matrix  $U_{spectralbands}$  defines a sparse vector for each spectral band that is theoretically invariant to illumination and subject variation. We show experimentally that when we significantly change the illumination condition between gallery and probe databases, values of these sparse vectors are subject to a small change that differs from one spectral band to another. We demonstrate theoretically that this change has a direct relation with the robustness of the corresponding spectral band to illumination variation, and is then exploited to select the best spectral bands for face matching over the IRIS-M<sup>3</sup> database.

The remainder of the paper is organized as follows: Section 2 briefly describes the IRIS-M<sup>3</sup> and DADL algorithm. In section 3 we details our approach for best spectral selection. Experimental results are displayed in section 4 and in section 5 we conclude our work.

## 2 The IRIS-M<sup>3</sup> Face Database and DADL Algorithm

### 2.1 IRIS-M<sup>3</sup> Face Database

In IRIS-M<sup>3</sup> face database [20], there are a total of 82 participants of different ethnicities, ages, facial, hair characteristics, and genders with a total number of

2624 face images. The image resolution is  $640 \times 480$  pixels and the interocular distance is about 120 pixels. The database was collected in 11 sessions between August 2005 and May 2006 with some participants being photographed multiple times. The subjects imaged are 76% male and 24% female; the ethnic diversity was defined as a collection of 57% Caucasian; 23% Asian (Chinese, Japanese, Korean, and similar); 12% Asian Indian; and 8% of African descents. For each subject, three groups of images have been captured, depending on the lighting conditions; a group of day lighted images, a group of halogen lighted images and a group of fluorescent lighted images. In turn, each image group was formed by two categories of images for each subject: a gray image and a multispectral image (image cube) formed by 25 spectral bands captured in the visible spectrum (from 480nm to 720nm) with a step of 10nm. For our experiments, day lighted images and halogen lighted images are matched against each other. We first evaluate the performance of our algorithms upon the gray images, then we enhance their performances using multispectral images.

## 2.2 Domain Invariant Dictionary Learning Algorithm

The Domain Invariant Dictionary Learning (DADL) algorithm is an algorithm that enables to decompose a 3-order face tensor  $\mathbb{T}$ , using 3-mode SVD, in the form of  $T = Z \times U_{subject} \times U_{spectralbands} \times U_{illumination}$ . The particularity of DADL is that the mode matrices  $U_{subject}$ ,  $U_{spectralbands}$ , and  $U_{illumination}$  are sparse matrices, i.e, most of their entries are zeros. The proposed algorithm begins by writing the decomposition of  $\mathbb{T}$  in the form of flattened matrices  $T_{(3)} = D_{(3)}^{T_1} \cdot U_{subject(3)}^{T_2} \cdot U_{spectralbands(3)}^{T_3} \cdot U_{illumination(3)}^{T_4}$ , where  $T_{i=1..4}$  are vector transpose operators that ensure the agree of dimensions between multiplied matrices. Then, two iterative algorithms are proposed to learn the base dictionary  $D$  and the sparse matrices  $U_{subject(3)} = [K_{i,j}] \in \mathbb{R}^{35 \times 35}$ ,  $U_{spectralbands(3)} = [S_{i,j}] \in \mathbb{R}^{25 \times 25}$ , and  $U_{illumination(3)} = [I_{i,j}] \in \mathbb{R}^{2 \times 2}$ . Hence, a new image  $y_{k,i}^s$  of subject  $k$  at illumination  $i$  and spectral band  $s$  could be written as  $y_{k,i}^s = D_{(3)}^{T_1} \cdot U_{subject(3)}^{T_2} \cdot U_{illumination(3)}^{T_3} \times S_s$ . where  $D_{(3)}^{T_1} \cdot U_{subject(3)}^{T_2} \cdot U_{illumination(3)}^{T_3}$  is the domain dictionary adapted to the spectral bands domain and  $S_s$  is the column vector number  $s$  of  $S$  corresponding to spectral band  $s$ . As we said,  $S_s$  determine the sparse decomposition of  $y_{k,i}^s$  on the spectral bands adaptive domain dictionary. The authors have shown that for the same spectral band  $s$ ,  $S_s$  is invariant when the subject  $k$  and/or the illumination  $i$  changes, i.e, the decomposition of an image  $y_{k,i_1}^s$ , captured at a different illumination  $i_1$  but for the same spectral band  $s$ , on the spectral bands domain adaptive dictionary  $D_{(3)}^{T_1} \cdot U_{subject(3)}^{T_2} \cdot U_{illumination(3)}^{T_3}$ , is the same, namely  $S_s$ . The same properties of domain invariance hold for the other domain matrices. Finally, the domain invariance property of DADL has a very interesting application for pose and illumination invariant face recognition.

### 3 Best Spectral Bands Selection Using Multilinear Sparse Decomposition

As shown by the authors of DADL (see Fig. 13 from [23]), and confirmed by our experimentations, the vector  $S_s$  varies slightly but continuously when varying the lighting condition. The authors of [23] considered this slight variation as a negligible error due to the iterative approximation process used by DADL to determine  $S_s$ . We show in this section that the error on  $S_s$  could be modeled as the sum of two errors: the mean square error  $dE$  due to the iterative process of DADL, and an error  $dK$  that quantifies the robustness of each spectral band against illumination variation. We propose to measure  $dK$  to determine the best spectral bands.

In the previous section, we got the following expressions:

$$\begin{aligned} y_{k,i}^s &= D_{(3)}^{T_1} \cdot U_{subject(3)}^{T_2,k} \cdot U_{illumination(3)}^{T_3,i} \times S_s \\ \Rightarrow S_s &= (D_{(3)}^{T_1} \cdot U_{subject(3)}^{T_2,k} \cdot U_{illumination(3)}^{T_3,i})^{-T} \cdot y_{k,i}^s \\ &= U_{illumination(3)}^{T_a,i} \cdot U_{subject(3)}^{T_b,k} \cdot D_{(3)}^{T_c} \cdot y_{k,i}^s \end{aligned} \quad (1)$$

Where  $T_a = T_1 \circ -T$ ,  $T_b = T_2 \circ -T$  and  $T_c = T_3 \circ -T$ . Then  $dS_s$  could be written as:

$$\begin{aligned} dS_s|_{illumination} &= d(U_{illumination(3)}^{T_a,i})|_{illumination} \cdot U_{subject(3)}^{T_b,k} \cdot D_{(3)}^{T_c} \cdot y_{k,i}^s \\ &+ U_{illumination(3)}^{T_a,i} \cdot d(U_{subject(3)}^{T_b,k})|_{illumination} \cdot D_{(3)}^{T_c} \cdot y_{k,i}^s \\ &+ U_{illumination(3)}^{T_a,i} \cdot U_{subject(3)}^{T_b,k} \cdot D_{(3)}^{T_c} \cdot d(y_{k,i}^s)|_{illumination} \end{aligned} \quad (2)$$

We define  $dE$  and  $dK$  as:

$$\begin{aligned} dE &= d(U_{illumination(3)}^{T_a,i})|_{illumination} \cdot U_{subject(3)}^{T_b,k} \cdot D_{(3)}^{T_c} \cdot y_{k,i}^s + \\ &U_{illumination(3)}^{T_a,i} \cdot U_{subject(3)}^{T_b,k} \cdot D_{(3)}^{T_c} \cdot d(y_{k,i}^s)|_{illumination} \\ dK &= U_{illumination(3)}^{T_a,i} \cdot d(U_{subject(3)}^{T_b,k})|_{illumination} \cdot D_{(3)}^{T_c} \cdot y_{k,i}^s \end{aligned} \quad (3)$$

Hence  $dS_s$  could be written as:

$$dS_s = dE + dK \Rightarrow dK = dS_s - dE \quad (4)$$

In Fig. 1, we determine the variation of  $dS$ ,  $dE$  and  $dK$ .  $dS$  is determined by varying the illumination and subjects (all combinations of illumination and subjects are considered) and measures the average error on  $S_s$ , while  $dE$  is determined by varying only the illumination and keeping the subjects and spectral bands fixed.  $dS$ ,  $dE$  and  $dK$  are determined for three spectral bands (SB) which are SB20 (at 670nm), SB24 (at 710nm) and SB25 (at 720nm). From Fig. 1 we can see that i)  $dK$  never become null (either for each combination (subject/illumination) or in average) and varies from one spectral band to another and that ii)  $dK$  is roughly

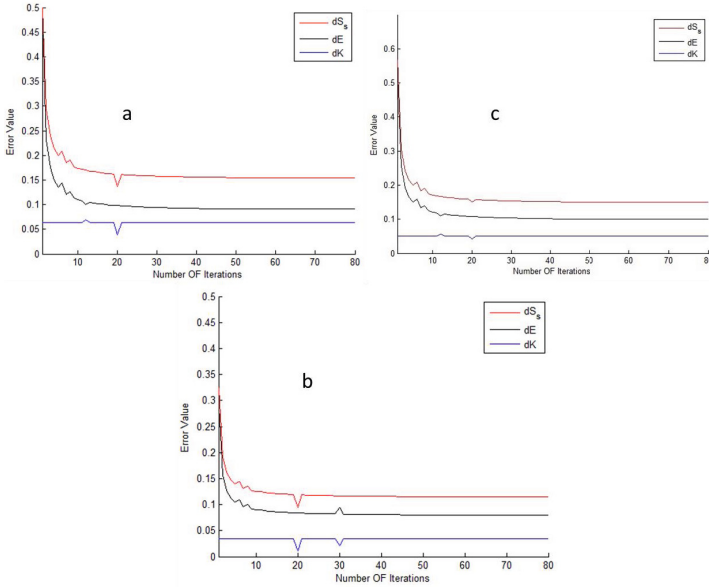


**Fig. 1.** Variation of different errors with the number of iterations for spectral bands a) SB24, b)SB25 and c)SB20

constant. Hence, the value of  $dK$  could be used to characterize spectral bands. On the other hand, the expression of  $dK$  is only function of  $d(U_{subject(3)}^{T_b,k})$ , and hence should become null whenever the same subject is used. This contradictory results between theory and experiments could be explained as follows: The traits of a given subject at a given spectral band are affected by illumination variation so that for a given recognition system, the identity of that subject is like being changed and hence  $d(U_{subject(3)}^{T_b,k})$  does not vanish. This explanation is consistent with the roughly constant value of  $dK$ ; the subject variation due to illumination happens only one time and without reversibility. Easily, we can see from the expression of  $dK$ , that the spectral band with the smallest  $dK$  is the less affected by illumination and hence the best for face recognition. we call  $dK$  the robustness to illumination factor or RIF. After computing the RIF of all spectral bands, we found out that *SB25* and *SB20* had the lowest RIF and were chosen as the best spectral bands for the studied illumination conditions. These results are consistent with those obtained by [21] and [22]. In the next section, selected spectral bands will be used to enhance the recognition performance of two state-of-the-art algorithms, which are MBLBP, and HGPP.

## 4 Experimental Results

In this section, two state-of-the-art algorithms are applied on images captured in the selected spectral bands SB25 and SB20 instead of usual braod band images. The aim of these experiments is to prove the efficiency of using multispectral

images to solve problems of high illumination variation. The distance  $D$  between two multispectral images  $I^p = (I_{SB25}^p, I_{SB20}^p)$  and  $I^g = (I_{SB25}^g, I_{SB20}^g)$  from the probe and gallery databases respectively, is computed as:

$$D(I^g, I^p) = \omega_{SB25} \cdot \|I_{SB25}^g - I_{SB25}^p\|_2 + \omega_{SB20} \cdot \|I_{SB20}^g - I_{SB20}^p\|_2 \quad (5)$$

$\omega_{SB25} = 0.035$  and  $\omega_{SB20} = 0.05$  are RIFs obtained for SB25 and SB20 respectively. The proposed approach with its two steps: best bands selection using RIF and spectral bands fusion at match score level using Eq 5, is compared to three other basic approaches which are : using broad band images  $X_{gray}$ , using randomly selected two spectral bands  $X_{two}$  (in our case we have chosen SB12 and SB19) and using all the 25 spectral bands  $X_{all}$  for face matching. The letter X designates the used algorithm (MBLBP or HGPP). For the multispectral images based approaches, each spectral band is weighted by its RIF and summed similarly as in Eq 5. CMC curves in Fig 2 and rank-1 recognition rates in Table 1 summarize the obtained results. we can see that using all or randomly chosen spectral bands gave bad results compared to using broad band images, while using selected best spectral bands gave the best performances. We conclude from this, that a multispectral images based face recognition system is inefficient and may be very time consuming, unless its preceded by a good system/phase for best spectral bands selection. Our approach has increased the recognition performance with 10% and 14% for MBLBP and HGPP algorithms respectively, which promote the use of multispectral images for illumination related problems in face recognition.

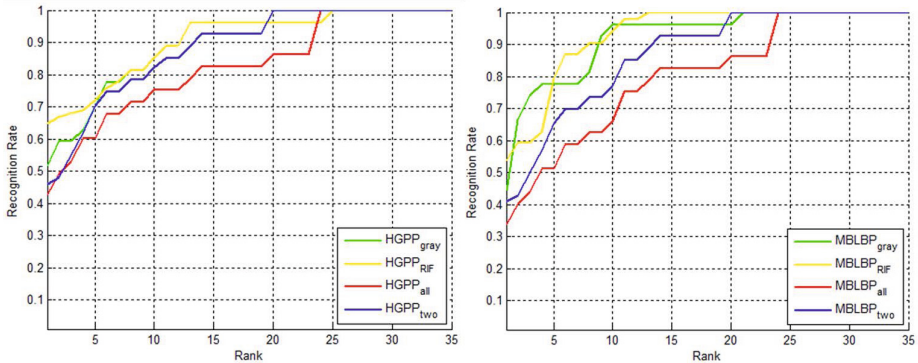


**Fig. 2.** CMC curves obtained for HGPP and MBLBP algorithms using different set of selected spectral bands

**Table 1.** Rank-1 recognition rates (%) of studied algorithms

	RIF	gray	two	all
HGPP	65	51	46	43
MBLBP	54	44	41	34

## 5 Conclusion

In this paper, we proposed a new approach for best spectral bands selection for face recognition. Multispectral images of 35 subjects presenting 25 different spectrums from 480nm to 720nm and three lighting conditions are grouped in a 3-mode face tensor  $T$  of size  $35 \times 25 \times 2$ .  $T$  is then decomposed using 3-mode SVD where three mode matrices for subjects, spectral bands and illuminations are sparsely determined. The  $25 \times 25$  spectral bands mode matrix contains a sparse vector for each spectral band that changes value with the change of illumination condition. We proposed to measure this change of sparse values to determine the robustness of each spectral band against high illumination variation presented by sun lighted images. Spectral bands with the lowest change in their sparse vectors are the less affected by illumination variation and hence were selected as the best spectral bands. Two spectral bands SB25 and SB20 at 720nm and 670nm respectively, were chosen by our approach as best spectral bands and were used to enhance the recognition performance of MBLBP and HGPP algorithms. An increase of accuracy of more than 11% have been registered for both algorithms compared to their performances on broad band images. These results highlighted the efficiency of multispectral images when they are coupled with an optimized system for best spectral selection. In future work, we plan to apply our algorithm on other multispectral images databases and investigate the different mode matrices provided by the multilinear decomposition approach.

**Acknowledgment.** This publication was made possible by NPRP grant # 4-1165-2-453 from the Qatar National Research Fund (a member of Qatar Foundation). The statements made herein are solely the responsibility of the authors.

## References

1. Smith, T.F., Waterman, M.S.: Identification of Common Molecular Subsequences. *J. Mol. Biol.* 147, 195–197 (1981)
2. May, P., Ehrlich, H.-C., Steinke, T.: ZIB Structure Prediction Pipeline: Composing a Complex Biological Workflow through Web Services. In: Nagel, W.E., Walter, W.V., Lehner, W. (eds.) *Euro-Par 2006*. LNCS, vol. 4128, pp. 1148–1158. Springer, Heidelberg (2006)
3. Foster, I., Kesselman, C.: *The Grid: Blueprint for a New Computing Infrastructure*. Morgan Kaufmann, San Francisco (1999)
4. Czajkowski, K., Fitzgerald, S., Foster, I., Kesselman, C.: Grid Information Services for Distributed Resource Sharing. In: 10th IEEE International Symposium on High Performance Distributed Computing, pp. 181–184. IEEE Press, New York (2001)
5. Foster, I., Kesselman, C., Nick, J., Tuecke, S.: *The Physiology of the Grid: An Open Grid Services Architecture for Distributed Systems Integration*. Technical report, Global Grid Forum (2002)
6. National Center for Biotechnology Information, <http://www.ncbi.nlm.nih.gov>
7. Zou, J., Ji, Q., Nagy, G.: A comparative study of local matching approach for face recognition. *Trans. Img. Proc.* 16(10), 2617–2628 (2007)

8. Ruiz-del Solar, J., Verschae, R., Correa, M.: Recognition of faces in unconstrained environments: A comparative study. *EURASIP J. Adv. Signal Process* 2009, 1:1–1:19 (2009)
9. Lei, Z., Liao, S., Jain, A.K., Li, S.Z.: Coupled discriminant analysis for heterogeneous face recognition. *IEEE Transactions on Information Forensics and Security* 7(6), 1707–1716 (2012)
10. Lei, Z., Pietikainen, M., Li, S.Z.: Learning discriminant face descriptor. *IEEE Transactions on Pattern Analysis and Machine Intelligence* 99, 1 (2013)
11. Chen, J., Yi, D., Yang, J., Zhao, G., Li, S.Z., Pietikinen, M.: Learning mappings for face synthesis from near infrared to visual light images. In: *CVPR*, pp. 156–163 (2009)
12. Zhang, B., Shan, S., Chen, X., Gao, W.: Histogram of gabor phase patterns (hgpp): A novel object representation approach for face recognition. *Trans. Img. Proc.* 16(1), 57–68 (2007)
13. Ahonen, T., Hadid, A., Pietikainen, M.: Face description with local binary patterns: Application to face recognition. *IEEE T-PAMI* 28, 2037–2041 (2006)
14. Vu, N.-S., Caplier, A.: Enhanced patterns of oriented edge magnitudes for face recognition and image matching. *IEEE T-IP* 21(3), 1352–1365 (2012)
15. Li, S.Z., Lei, Z., Ao, M.: The hfb face database for heterogeneous face biometrics research. In: 6th IEEE Workshop on Object Tracking and Classification Beyond and in the Visible Spectrum (OTCBVS, in conjunction with CVPR 2009), pp. 1005–1010 (2009)
16. Shao, T., Wang, Y.: The face images fusion based on laplacian pyramid and lbp operator. In: 9th International Conference on Signal Processing, pp. 1165–1169 (2008)
17. Chang, H., Koschan, A., Abidi, B.: Fusing continuous spectral images for face recognition under indoor and outdoor illuminants. *Machine Vision and Application* 19(4), 1432–1769 (2008)
18. Buysseens, P., Revenu, M.: Ir and visible face identification via sparse representation. In: 2010 Fourth IEEE International Conference on Biometrics: Theory Applications and Systems (BTAS), pp. 1–6 (2010)
19. Mangai, U., Samanta, S., Das, S., Chowdhury, P.R.: A survey of decision fusion and feature fusion strategies for pattern classification. *IETE Tech. Rev.* 27, 293–307 (2010)
20. Chang, H., Yao, Y., Koschan, A., Abidi, B., Abidi, M.: Improving face recognition via narrowband spectral range selection using jeffrey divergence. *Trans. Info. For. Sec.* 4(1), 111–122 (2009)
21. Bouchech, H.J., Foufou, S., Koschan, A., Abidi, M.: Studies on the effectiveness of multispectral images for face recognition: Comparative studies and new approaches. In: *Proceeding of the IEEE SITIS Conference, Kyoto, Japan* (2013)
22. Bouchech, H.J., Foufou, S., Koschan, A., Abidi, M.: Dynamic best spectral bands selection for face recognition. To appear in the *Proc. of the 48 International Conference on Information Sciences and Systems (CISS 2014), Princeton, NJ, USA, March 19-21* (2014)
23. Qiu, Q., Chellappa, R.: Compositional Dictionaries for Domain Adaptive Face Recognition. *CoRR abs/1308.0271* (2013)